ELSEVIER
Energy Conversion and Management xxx (2004) xxx–xxx
ENERGY CONVERSION & MANAGEMENT
www.elsevier.com/locate/enconman

Transient cooling of thermoelectric coolers and its applications for microdevices

Ronggui Yang [a,*], Gang Chen [a], A. Ravi Kumar [b], G. Jeffrey Snyder [c], Jean-Pierre Fleurial [c]

[a] *Mechanical Engineering Department, Massachusetts Institute of Technology, Room 7-042, 77 Mass. Ave, Cambridge, MA 02139, USA*
[b] *Allegro MicroSystems, Inc., 115 NE Cutoff Worcester, MA 01606, USA*
[c] *Jet Propulsion Laboratory, California Institute of Technology, Pasadena, CA 91109, USA*

Received 3 April 2004; received in revised form 15 July 2004; accepted 18 July 2004

Abstract

If a current pulse with a magnitude several times higher than the steady state optimum current is applied to a thermoelectric cooler, an instantaneously lower temperature than that reachable at the steady state can be obtained. Most previous studies of this transient cooling effect focus on the minimum temperature achievable for free standing thermoelectric (TE) elements. In this work, we systematically study the transient response of thermoelectric coolers with and without mass loads through examination of both the minimum temperature reached and the time constants involved in the cooling and the recovering stages. For integrated thermoelectric-passive mass load systems, two distinguishable cooling regimes, uniform cooling and interfacial cooling, are identified, and the criterion for utilization of the transient cooling effect is established based on the time constants. Although the results of this work are generally applicable, the discussions are geared towards cooling of microdevices that are of current interests.

Keywords: Thermoelectric; Thermal management; Transient cooling; Microdevice; Thermoelectric cooler

* Corresponding author. Tel.: +1 617 253 3555; fax: +1 617 253 3484.
E-mail address: ronggui@mit.edu (R. Yang).

0196-8904/$ - see front matter
doi:10.1016/j.enconman.2004.07.004

Nomenclature

A	cross-sectional area (m^2)
A_0	constant introduced in Eq. (5)
B	constant introduced in Eq. (15)
ρc_p	volumetric heat capacity (J/m^3 K)
j	applied current density (A/m^2)
j_0	optimum applied current density (A/m^2)
k	thermal conductivity (W/m K)
l	length (m)
l_c	critical dimension of cooling target for using interfacial cooling (m)
P	normalized pulse magnitude
S	Seebeck coefficient (V/K)
t	time (s)
t_α	diffusion time constant (s)
t_m	time to reach minimum temperature (TRM) (s)
t_h	holding time (s)
T	temperature (K)
T_1	minimum steady state temperature at cold junction (K)
x	coordinate
Z	figure of merit (K^{-1})
Z'	reduced figure of merit of integrated system as defined in Eq. (15) (K^{-1})

Greeks

α	thermal diffusivity (m^2/s)
ρ	electrical resistivity (Ω m)
ξ	effusivity ratio $[=(k\rho C_p)_L/(k\rho C_p)]$
ζ	constant introduced in Eq. (16)

Subscripts

c	cold end of TE cooler
h	hot end of TE cooler
l	cooling object of integrated system
SS	steady state
t	transient

1. Introduction

The Peltier effect in a thermoelectric (TE) device is a local effect confined to the junctions of the thermoelectric elements while the Joule heating occurs volumetrically over the thermoelectric elements. At steady state conditions, these two effects, combined with heat conduction from the hot end to the cold end, determine the cold side temperature. The cooling coefficient of performance and maximum temperature drop depend on the properties of the thermoelectric materials through the figure of merit, $Z = S^2/\rho k$, where S is the Seebeck coefficient, ρ is the electrical resistivity and k is the thermal conductivity. If a current pulse with a magnitude several times higher than the steady state optimum current j_0 , which is the current to obtain the minimum steady state cold side temperature, is applied to the element, an instantaneously lower temperature than that reachable at the steady state can be achieved at the cold end because of the delay of the thermal diffusion of the volumetric Joule heat. This phenomenon is referred to as the transient thermoelectric effect [1].

After Stilbans and Fedorovich [2] first reported the transient cooling effect in thermoelectric (TE) elements, the phenomenon has been extensively investigated [3–14]. To obtain larger transient cooling temperature differences, measured by the additional temperature drop at the cold junction caused by the transient current, various approaches have been taken, such as applying a non-square transient current [4], using thermoelectric elements with variable cross-sectional area [11] and surface junction [12].

Recent developments in the fabrication of thermoelectric microcoolers make it possible to place the TE microcoolers near the high heat flux producing regions of electronic or optoelectronic devices that need to be cooled [15–18]. This will enable compact thermal systems for device and package level cooling. The transient cooling effect in thermoelectric coolers might be employed to improve the performance of these devices further [10,13,14]. The results of the previously mentioned studies on transient cooling are not directly applicable to the microcoolers because those studies are extensively for free standing bulk thermoelectric elements and most of them focused only on the maximum transient temperature difference, i.e. the minimum temperature achievable. Several issues that are of particular importance for microdevices need to be addressed. First of all, several time constants, the time to reach minimum temperature (TRM) and the time to remain at minimum temperature (holding time), are very important for characterization and utilization of the transient cooling effect since the effect can only be sustained for a limited time. In parallel of this work, Snyder et al. [10] established theoretically and experimentally the essential parameters that describe the transient cooling effect using a square pulse, such as the minimum temperature achieved, the maximum temperature overshoot, the TRM, the holding time and the time between pulses. Semi-empirical relationships are established for the dependence of these parameters on the current pulse amplitude, thermoelectric element length, thermoelectric figure of merit and thermal diffusivity. In Section 2 of this paper, we systematically studied the dependence of the minimum achievable temperature and the time to reach minimum temperature on the current pulse amplitude, thermoelectric element length, applied current shape and the TE element geometry using the finite difference method for a free standing TE element. Since the object to be cooled is a passive mass load for the thermoelectric coolers, it affects the minimum temperature achievable, particularly when the object to be cooled is comparable to the TE coolers in size, as is often the case for microcoolers. In Section 3, we present the performance analysis of the cooling object and microthermoelectric cooler integrated system. Two distinguishable cooling regimes (uniform cooling and interfacial cooling) are identified, and the criterion for utilization of the transient cooling effect is established based on the time constants.

2. Free standing thermoelectric element

In this section, we evaluate the performance of a freestanding TE element. This serves as a basis for analyzing the minimum temperature that can be obtained during the transient mode operation and also sets the limit for an integrated TE-load system discussed in Section 3. In steady state operation of the TE device, the effect of the applied current magnitude on the device performance is well understood. However, during the transient mode, operation parameters such as applied current pulse shape and pulse amplitude severely affect the performance of the device. Another constraint that affects operation of the TE device during transient operation is the geometry of the TE element. Geometry parameters like the length of the element and cross-sectional area of the cold and hot ends particularly affect the thermal diffusion to and away from the ends of the TE element.

2.1. Finite length thermoelectric element with square pulse

The theoretical analysis of the transient cooling of a free standing TE element can be approximated into a one-dimensional problem as shown in Fig. 1(a) by assuming the n-type and p-type thermoelectric elements have exactly the same properties except for the opposite sign of the Seebeck coefficient. The differential equation is

$$\frac{\partial^2 T}{\partial^2 x^2} + \frac{j^2 \rho}{k} = \frac{1}{\alpha}\frac{\partial T}{\partial t}, \tag{1}$$

where a is the thermal diffusivity, ρ is the electrical resistivity, k is the thermal conductivity, j is the applied current density and T is temperature. The lowest temperature is achieved when there is no external heat load onto the TE element, i.e. at $x = 0$,

$$-k\frac{\partial T}{\partial x} + SjT = 0. \tag{2}$$

We further assume that the hot side is maintained at a constant heat sink temperature, i.e. at $x = l$, where l is the length of the thermoelectric elements,

$$T(x = l, t) = T_{\mathrm{h}}. \tag{3}$$

When the right-hand side of Eq. (1) equals 0, we obtain the steady state temperature distribution $T_{\mathrm{SS}}(x)$

$$T_{\mathrm{SS}}(x) = T_{\mathrm{c}} + (T_{\mathrm{h}} - T_{\mathrm{c}})(2x/l - x^2/l^2), \tag{4}$$

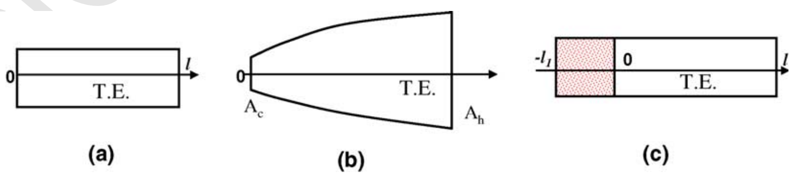

Fig. 1. Schematic drawing: (a) free standing TE element, (b) axisymmetric TE element with variable cross-sectional area (cf. Section 2.3) and (c) cooling object and micro TE cooler integrated system (cf. Section 3).

where T_c is the cold junction temperature. The solution to the steady state problem for a material with Z independent of temperature [1] leads to the maximum steady state temperature difference $T_{\max} = T_h - T_1 = ZT_1^2/2$, where T_1 is the minimum steady state cold side temperature at $j_0 = \alpha T_1/\rho l$. After the initial steady state temperature distribution is obtained, the current is suddenly increased to j_t to obtain the transient cooling. We define a normalized pulse magnitude P as $P = j_t/j_0$ for a square pulse. After the cold junction temperature increases back to its steady state value T_1, the current is switched back to its optimum steady state value j_0. Fig. 2 shows the numerical simulation of the cold junction temperature in a typical transient cycle. Also shown are the definitions of several time constants. The holding time, which is the period to keep the cold side temperature below a certain temperature, depends on its application limit. The recovery period is the time required for the TE element to reach its steady state temperature after removing the applied transient current, and the steady state optimum current is applied as shown in Fig. 2.

Babin and Iordanishvili [6] analyzed the transient response of free standing TE elements and found that for currents that are at least twice as large as the steady state optimum current j_0 , it is a reasonable approximation to treat the TE element as a semi-infinite body because the TRM is small compared to the diffusion time constant for a large transient pulse $t_\alpha = l^2/\alpha$. They showed that the transient cooling effect $\Delta T_t = T_1 - T_2$, where T_2 is the minimum transient temperature of the cold side, does not depend on the TE element length when the TE element is longer than $3\sqrt{\alpha t_m}$. The time to reach the minimum temperature (TRM) t_m can be approximated as

$$t_m = A_0^2(k\rho c_p)/(j^2S^2), \tag{5}$$

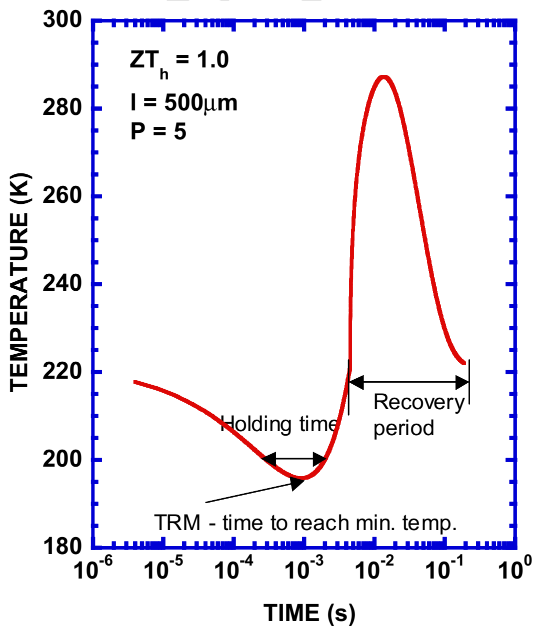

Fig. 2. The change of the cold junction temperature with time in a typical transient cycle and the definition of time constants.

where A_0 is determined by the properties of the TE elements and can be determined by:

$$ZT_1 = \frac{1}{\gamma}\frac{\sqrt{\pi}A_0\exp A_0^2\mathrm{erfc}A_0}{1-\sqrt{\pi}A_0\exp A_0^2\mathrm{erfc}A_0} \tag{6}$$

Our numerical simulation confirms that the transient cooling effect $\Delta T_t = T_1 - T_2$ (where T_2 is the minimum transient temperature) does not depend on the TE element length. Fig. 3(a) compares the numerical solution of the maximum cooling effect with the model by Babin and Iordanishvili [6]. The model agrees well with the numerical solution for large current pulse. A simplified model by linearization of the transient term in Eq. (1) has been established and documented in [10]. Although the length does not have much effect on the minimum transient temperature for free standing TE elements for a given transient pulse as shown in Fig. 4(a), it determines the thermal inertia of the TE elements. This indicates that the length of a TE element affects the holding time as well as the recovery period. For easy comparison, we have defined the holding time as the time period over which it is possible to maintain the temperature within the range of 2 K (the choice of 2 K is arbitrary as stated before) from the lowest temperature possible in this section. Fig. 4 shows the holding time (Fig. 4(b)) as a function of TE element length for different normalized pulse magnitudes and the duty cycle (Fig. 4(c)), which is defined as the percentage of the holding time over the recovery period. As shown in Figs. 4(a) and (b), the holding time is longer as the length of the element increases. This is because the applied current flux is much larger for shorter elements, and thus, ther is high heat dissipation density close to the cold junction, for example the applied current pulse ($5\times j_0$) for the 50 μm element is ten times larger than that of the 500 μm

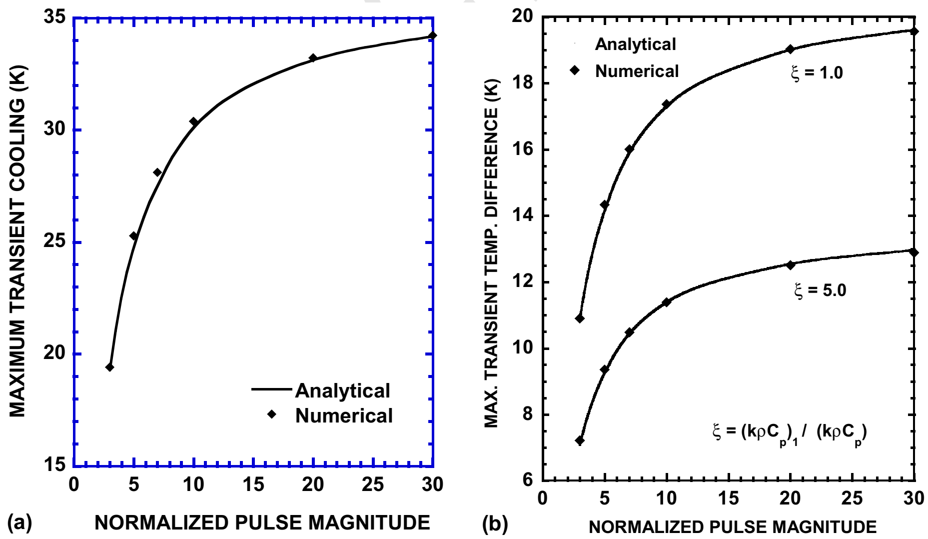

Fig. 3. (a) Comparison of the maximum transient temperature difference obtained by numerical simulation with the model by Babin and Iordanishvili [6] and (b) the maximum transient temperature difference of the semi-infinite integrated system as a function of the normalized pulse magnitude of applied transient current and the effusivity ratio $\xi = (k\rho C_p)_1/(k\rho C_p)$ (cf. Section 3.1) Results of analytical model are compared with numerical simulation.

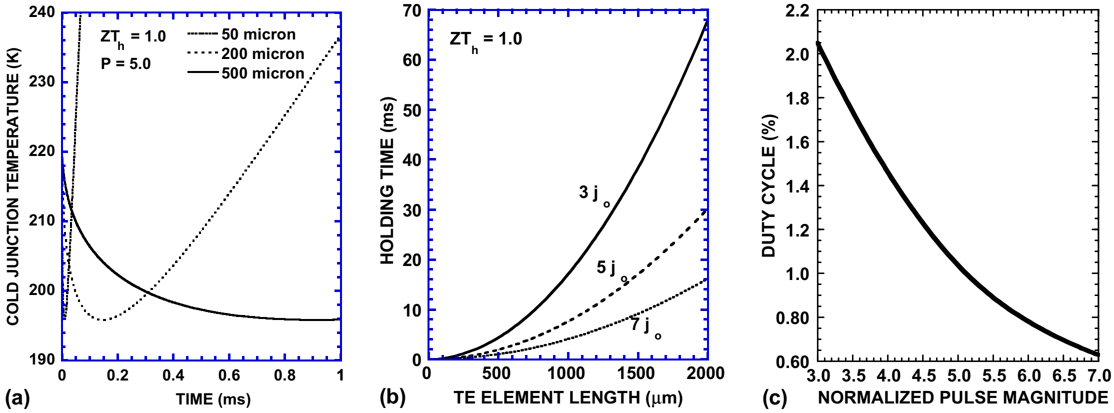

Fig. 4. (a) Cold junction temperature of different thermoelectric element length under same applied transient current shows that the minimum cold side temperature achievable is approximately the same for various TE element lengths, (b) the holding time as a function of TE element length for different normalized pulse magnitudes and (c) the duty cycle. Here, the holding time is defined as the time period over which it is possible to maintain the temperature within the range of 2 K from the lowest temperature possible.

element. However, the recovery period will be longer for the longer element and vice versa. This results in the duty cycle not being a function of the TE element length but being a function of the magnitude of the transient pulse only.

2.2. Pulse shape effect

The current pulse shape also affects the transient response. Using the variational method, Landecker and Findlay [4] concluded that the transient temperature would approach absolute zero with temperature independent thermal and thermoelectric properties, provided that the current were allowed to rise indefinitely. No one has been able experimentally to demonstrate this by far. Fig. 5 shows the temperature response for three different pulse shapes for a 0.5 mm TE element obtained from numerical simulations. We found that the lowest temperature that can be obtained is approximately the same for any pulse shape, but the holding time differs for different pulse shapes. In order to take advantage of the spatial difference between the Peltier and Joule effects, a better approach would be that the applied current pulse should be higher at the beginning, and subsequently, it should be reduced, similar to the pulse $j = t^{-0.5}$. This will enable a longer holding time compared to a ramp pulse or the square pulse, as shown in Fig. 5.

2.3. Effects of TE element shape

It has been known that the minimum temperature achievable by a TE device in steady state does not depend on the shape, but it has been conjectured that the TE element shape might have an effect on the transient performance of thermoelectric devices [11]. The cross-sectional areas of the hot end A_h and cold end A_c determine the thermal resistance for the Joule heat. By increasing the ratio of A_h to A_c, Hoyos et al. [7] experimentally showed that it is possible to obtain better

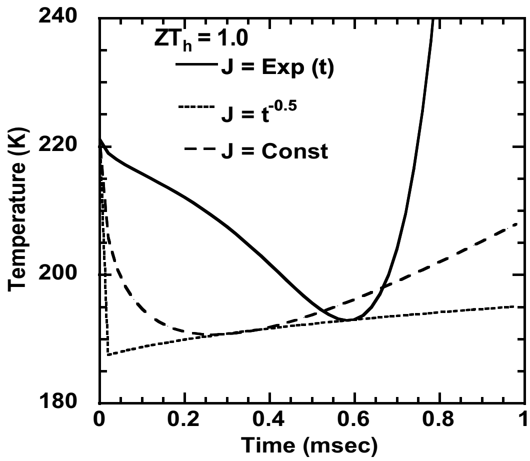

Fig. 5. Cold junction temperature response for three different pulse shapes for a 0.5 mm TE element.

transient performance, i.e. lower temperature and shorter recovery time after turning off the transient pulse, compared to TE elements having equal cross-sectional area. In microfabricated devices, the TE legs might not be straightly vertical, as in electrodeposition of thermoelectric microdevices [16]. However, rigorous theoretical study on the TE element shape effect on the transient cooling effect has yet to be reported. This section presents numerical results on the effects of leg shape on the transient cooling performance. Again, the analysis here is based on the assumption that the thermoelectric properties are independent of temperature and the contact resistance is negligible.

For axisymmetric TE elements with variable cross-sectional area as shown in Fig. 1(b), the governing differential equation should be written as

$$\frac{1}{\alpha}\frac{\mathrm{d}T}{\mathrm{d}t} = \frac{I^2\rho}{kA^2(x)} + \frac{1}{A(x)}\frac{\mathrm{d}A(x)}{\mathrm{d}x}\frac{\mathrm{d}T}{\mathrm{d}x} + \frac{\mathrm{d}^2T}{\mathrm{d}x^2}, \tag{7}$$

where I is the total current flow through cross-sectional area $A(x)$. The shape effect is reflected by the second term of the right-hand side of Eq. (7). The results presented below are for tapered axisymmetric TE legs with the cross-sectional area changing linearly with the TE leg length,

$$A(x) = A_c\left(1 + \frac{A_h - A_c}{A_c}\frac{x}{l}\right), \tag{8}$$

where A_c is the cross-sectional area at the cold end $x = 0$ and A_h is the cross-sectional area at the hot end $x = l$. Similar to the cylindrical TE elements, the maximum transient temperature difference and the holding time for the tapered axisymmetric TE elements also do not depend on the absolute value of the cross-sectional area. Fig. 6(a) shows the normalized holding time and the minimum cold side temperature with different area ratio of the cold end and the hot end. The holding time is normalized to that of the cylindrical TE leg whose cross-sectional area is the same as the average area of the tapered element. The tapered leg makes the thermal resistance asymmetric, and the Joule heat will preferentially be conducted towards the end that has the larger cross-

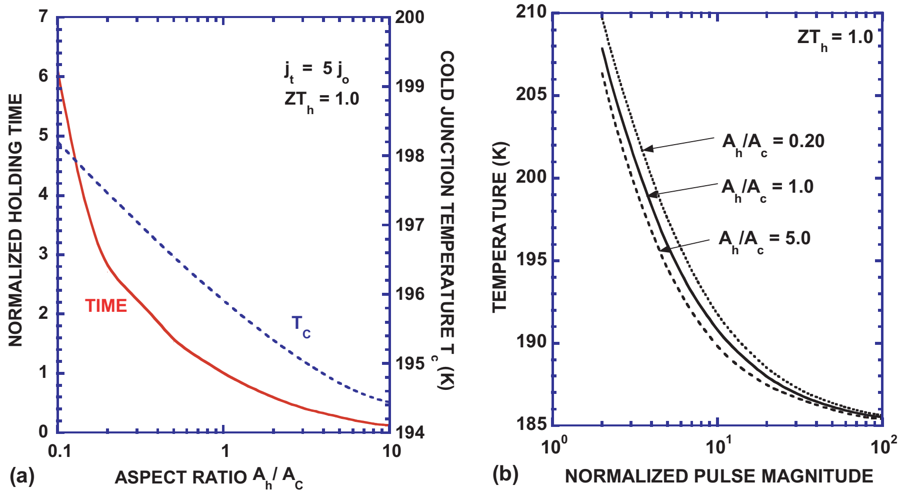

Fig. 6. Transient performance of tapered axisymmetric thermoelectric legs: (a) normalized holding time and minimum temperature as a function of the area ratio, (b) the applied current effect on the minimum temperature for various area ratios of shaped TE cooler.

sectional area. However, more Joule heat is generated close to the end that has the smaller cross-sectional area. The competition between these two effects results in a lower minimum transient temperature for the tapered axisymmetric thermoelectric legs with smaller cross-sectional area at the cold end. However, the holding time is decreased by several times for such tapered thermoelectric legs with the smaller cross-sectional area at the cold end. The increase of holding time of those TE legs with larger cross-sectional area at the cold end can potentially be useful for the device to be operated for a longer time. Fig. 6(b) shows the minimum transient temperature as a function of the magnitude of the applied transient current and the area ratio.

3. Response of integrated thtermoelectric-passive load system

In applications, it is expected that an additional mass (i.e, the object to be cooled) be attached to the TE element. The performance of such an integrated system differs from that of the stand alone TE elements. The thermal properties of the attached mass can severely affect the transient performance of the integrated system. Here, we focus discussion particularly on important properties such as thermal conductivity, heat capacitance and density. We begin our analysis with a system that consists of a semi-infinite object to be cooled that is attached to a semi-infinite TE element. Later, the discussion is extended to a more realistic situation where a finite length object is attached to a finite length TE element. No active heat generation is assumed in the load.

The object to be cooled can be treated as a passive mass load attached to a thermoelectric element when contact resistance is neglected. Fig. 1(c) shows the schematic configuration of an integrated TE-load system. The governing equation for heat conduction in the loaded mass $(-l_1 < x < 0)$ is

$$\frac{\partial^2 T}{\partial^2 x^2} = \frac{1}{\alpha_1}\frac{\partial T}{\partial t}. \tag{9}$$

The subscript 1 denotes the cooling object. The boundary conditions at the interface between the cooling object and the TE element are

$$-k_1\frac{\partial T}{\partial x} = -k\frac{\partial T}{\partial x} + SjT, \tag{10}$$

$$T(0^-, t) = T(0^+, t). \tag{11}$$

The other end of the attached mass is insulated, thus

$$\frac{\partial T}{\partial x}\Big|_{x=-l_1} = 0. \tag{12}$$

3.1. Transient response of semi-infinite integrated systems

In a previous study [13], we analyzed the transient temperature difference based on the assumption that both the TE element and the object to be cooled are semi-infinite and maintained at room temperature. In a real situation, the TE element must be maintained at its optimum steady state before an additional transient current is applied. The initial temperature distribution of the TE element degrades the transient temperature difference predicted in [13] and should be taken into account. That is, the new initial condition should be written as

$$\begin{cases} T(x) = T_{\mathrm{h}} - (T_{\mathrm{h}} - T_1)\left(1 - \dfrac{x}{l}\right)^2, & l > x > 0, \\ T(x) = T_1, & -l_1 < x < 0. \end{cases} \tag{13}$$

Following the same technique as in [13] and taking into account the initial steady state temperature distribution, we obtain the following analytical solution for the transient temperature difference ΔT_{t} for a square pulse:

$$\begin{aligned} \Delta T_{\mathrm{t}} = \left[1 - \frac{\gamma'}{P}\right] \cdot \Bigg\{ T_1\left[(1 - \exp B^2 \mathrm{erfc} B)\cdot\left(\frac{1}{Z'T_1} + \frac{1-\gamma'}{1-\gamma'/P}\right) - \frac{2B}{\sqrt{\pi}Z'T_1}\right] \\ - \frac{k_1/\sqrt{\alpha_1}}{k_1/\sqrt{\alpha_1} + k/\sqrt{\alpha}} \cdot \frac{1}{Z'}\left[1 - \exp B^2 \mathrm{erfc} B - \frac{2B}{\sqrt{\pi}}\right]\Bigg\}, \end{aligned} \tag{14}$$

where

$$\gamma' = \frac{2(T_{\mathrm{h}} - T_1)}{T_1(\sqrt{1 + 2ZT_{\mathrm{h}}} - 1)P}, \quad Z' = Z\frac{k^2/\alpha}{\left(k/\sqrt{\alpha} + k_1/\sqrt{\alpha_1}\right)^2}, \quad B = \frac{Sj\sqrt{t}}{k/\sqrt{\alpha} + k_1/\sqrt{\alpha_1}}. \tag{15}$$

The condition for maximum ΔT_{t} is obtained when $B = B_0$ satisfies

$$Z'T_1 = \frac{[1 - (k_1/\sqrt{\alpha_1})/(k/\sqrt{\alpha} + k_1/\sqrt{\alpha_1})]}{\zeta}\,\frac{\sqrt{\pi}B_0 \exp B_0^2 \mathrm{erfc} B_0}{1 - \sqrt{\pi}B_0 \exp B_0^2 \mathrm{erfc} B_0}, \tag{16}$$

where $\zeta = \frac{1-\gamma'}{1-\gamma'/P}$.

The effect of the initial temperature distribution is reflected in γ'. Eq. (14) shows that the initial temperature distribution indeed reduces the additional temperature drop derived in [13].

Fig. 3(b) shows the maximum transient temperature difference of the semi-infinite integrated system as a function of the magnitude of the applied transient current and the effusivity ratio $\xi = (k\rho C_p)_1/(k\rho C_p)$. With the mass attached at the cold end, the cooling power produced diffuses into the cooling object, which degrades the additional temperature drop compared to the free standing TE element. It shows that a decrease in the value of the effusivity of the object to be cooled helps in decreasing the thermal diffusion into the object and, hence, achieving a larger maximum transient temperature difference. This partial cooling of the object might be attractive for some applications such as cooling the active region of a semiconductor laser rather than the whole substrate. The model is also compared with numerical simulation results. The analytical model agrees well with the numerical simulation in the semi-infinite regime.

3.2. Integrated system with finite length TE element

In practical applications, the cooling object and the TE element integrated system might behave neither like a free standing TE element nor like a semi-infinite integrated system. The transient temperature response of a practical integrated system with finite length depends on not only the transient current but also the length and the thermal properties of the object to be cooled and TE elements. Since general analytical solutions for such cases are difficult, a numerical method is used to study the transient effect for a practical integrated load and TE cooler system as shown in Fig. 1(c). In addition, experiments were conducted on a system as shown in the inset of Fig. 7. It consists of two 1 mm × 1 mm × 6 mm Bi_2Te_3 thermoelectric legs soldered by a 3.5 mm × 2.5 mm copper sheet that is 35 μm thick. The details of such experimental studies are reported in [10]. Fig. 7 compares the numerical simulation results with experimental data. Copper is treated as the cooling object and the properties used were obtained by fitting the steady state response of the TE element. To treat the system as 1D problem, the length of the copper stub is equivalent to a length of 153 μm with the same cross-sectional area while considering the high thermal conductivity of copper. $k_1 = 350$ W/(m K) and $(\rho c_p)_1 = 1.20 \times 10^6$ J/m^3 K are used for the copper properties. The properties of Bi_2Te_3 are fitted as: $(\rho c_p) = 1.20 \times 10^6$ J/m^3 K, $k = 1.20$ W/(m K), $S = 235$ μV/K , $ZT_{300\ \mathrm{K}} = 0.706$. Fig. 7 shows that the numerical model developed here can be used to predict the transient response. The deviation between the experimental data and the simulation results in Fig. 7 after the transient pulses are turned off is due to the thermal resistance of the hot side heat sink, which is not considered in our current model.

Fig. 8(a) shows the effect of thermal conductivity on the maximum transient temperature difference. It shows that the thermal conductivity does not have much effect on the maximum transient temperature difference when l_1/l is small, where l_1 is the length of the cooling object and l is the length of the TE element. This means that the attached cooling object is cooled uniformly because the transient cooling power diffuses effectively to the whole cooling object. As the length ratio l_1/l increases, the maximum transient temperature difference becomes independent of the length ratio because both sides can be treated as semi-infinite. In this case, however, the thermal conductivity of the load affects the maximum temperature difference. A high load thermal conductivity leads to a smaller transient cooling effect due to the larger heat spreading in the load side. Fig. 8(b) shows the effect of the volumetric heat capacity on the maximum transient temperature

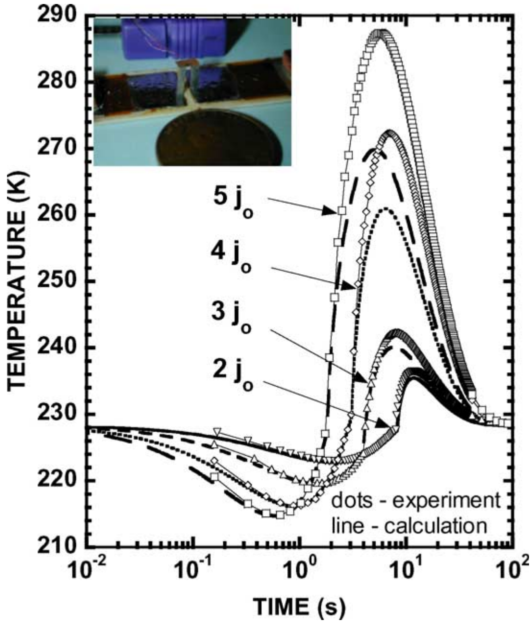

Fig. 7. Comparison of numerical simulation and experimental results (line—numerical results, dots—experimental results). The inset shows the configuration of the experimented TE cooler. It consists of two 1 mm × 1 mm × 6 mm Bi_2Te_3 thermoelectric legs soldered by a 3.5 mm × 2.5 mm copper sheet that is 35 μm thick.

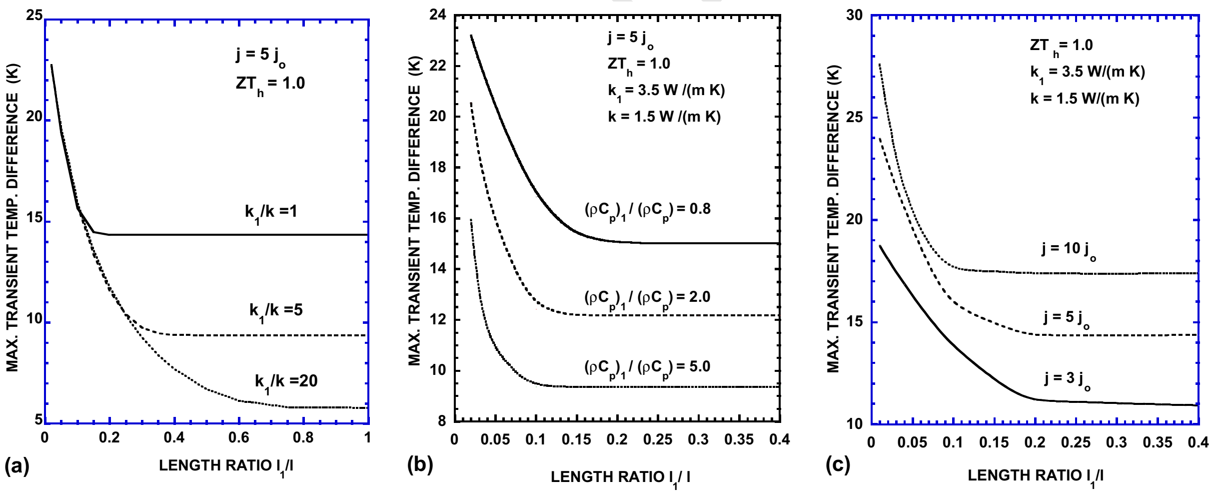

Fig. 8. The maximum transient temperature difference of integrated systems as a function of the length ratio: (a) thermal conductivity effect, (b) heat capacity effect and (c) applied current effect.

difference. The maximum transient temperature difference increases when decreasing the heat capacity of the cooling object for any length ratio. Fig. 8(c) shows the effect of the applied transient current on the maximum transient temperature difference. All three figures show a flat region of the maximum transient temperature difference when l_1/l is larger than a certain value. This is the interfacial cooling region. In this regime, the thermoelectric legs and the passive load can be treated as semi-infinite. The maximum transient temperature difference does not change with the length ratio but depends on the thermal conductivity or thermal effusivity ratio. In the other limit, the uniform cooling regime, the thermal conductivity of the load does not affect the maximum transient temperature difference. The maximum transient temperature difference is a function of the thermal mass ratio of the load to the thermoelectric elements. In the uniform cooling regime, the transient response can be modeled as a small attached mass system.

Fig. 9(a) shows that different cooling objectmicro TE element (Bi_2Te_3) integrated systems might fall in different cooling regimes under the transient pulse. The conductivity of the cooling object has been chosen to be $k_1 = 3.5$ W(m K), which mimics the active region of the InAs/AlSb mid-IR laser. For a given integrated system, the transient cooling might change from uniform cooling to interfacial cooling if the applied current increases substantially. For a small normalized pulse magnitude P, the cooling object is cooled uniformly and the cooling effect follows similarly to 3(a), i.e. the system can be treated as a free standing TE element with a very small attached mass, if the TE element is long enough that the holding time is much larger than the thermal diffusion time to the other end of the cooling object. The holding time decreases with the normalized pulse magnitude P. For a large normalized pulse magnitude P, the holding time is shorter than the thermal diffusion time to the other end of the cooling object, and the transient effect is confined to the interface region. In both extremes, the cold junction temperature decreases with increasing pulse magnitude. In the transition regime, the competition between the localized cooling at the interface and the cooling power diffused into the loaded mass results in the increase of the cold junction temperature with increasing pulse. Fig. 9(b) is to illustrate these arguments. It shows the transient cooling effect in a 75 μm cooling object—1000 μm Bi_2Te_3 integrated system. Uniform cooling

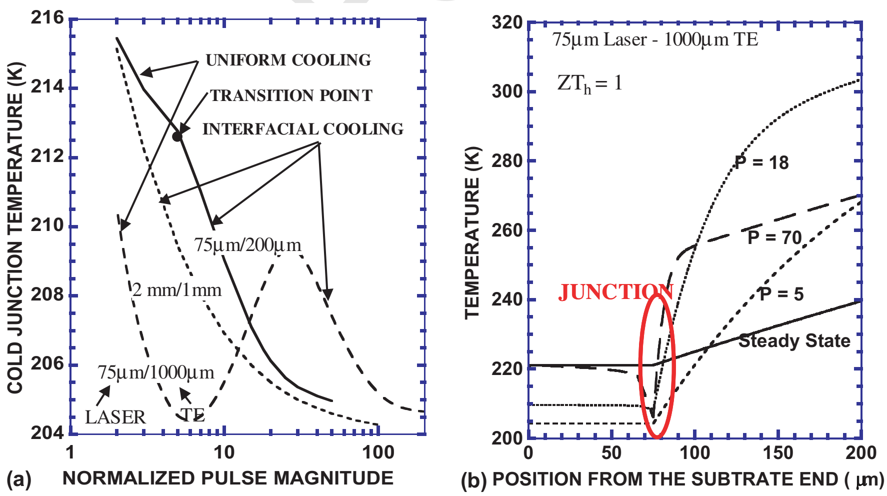

Fig. 9. (a) Two cooling regimes are observed depending on the length ratio of the cooling object micro TE element (Bi_2Te_3) integrated system and the applied transient current and (b) the transient cooling effect in a 75 μm cooling object—1000 μm Bi_2Te_3 integrated system: Uniform cooling occurs at $P = 5$, and interfacial cooling occurs at $P = 70$.

occurs at $P = 5$, and interfacial cooling occurs at $P = 70$. The temperature profile for $P = 18$ shows the competition of localized cooling at the interface and the cooling power diffusion into the loaded mass.

Lumped analysis shows that the holding time t_h of an integrated system, which is defined as the time that the cold junction is maintained below the steady state minimum temperature, is

$$t_h = \frac{1}{(P+1)^2}\frac{l^2}{\alpha} \tag{17}$$

which is around four times as long as the TRM [10]. This holding time expression is approximately valid for both free standing TE elements and integrated cooling systems. To utilize the transient cooling effect in a uniform cooling mode, the holding time must be larger than the diffusion time, which is the time required for the transient cooling effect to diffuse from the interface to the other end of the object to be cooled. Comparing the scale of the holding time and the diffusion time, we found that the criterion for utilizing the transient cooling effect is

$$\frac{l_1}{l} < \frac{1}{P+1}\sqrt{\frac{\alpha_1}{\alpha}}. \tag{18}$$

In other words, when $l_1 > \frac{l}{P+1}\sqrt{\frac{\alpha_1}{\alpha}}$, the integrated system can be treated as a semi-infinite system, and the maximum transient temperature difference can be predicted by Eq. (1). To utilize interfacial cooling, the critical dimension l_c of the cooling target should satisfy $l_c < \frac{l}{P+1}\sqrt{\frac{\alpha_1}{\alpha}} < l$.

4. Conclusions

The transient cooling effect should be characterized by both the minimum temperature and several time constants, such as the time to reach the minimum temperature (TRM) and the holding time. We systematically studied the effects on the transient cooling performance of the current pulse amplitude, thermoelectric element length, applied current shape and the TE element geometry using primarily the finite difference method. Because the cooling object is a passive mass load, it will affect the transient performance. The performance of the cooling object and micro TE element integrated system are analyzed. Two distinctive cooling regimes (uniform cooling and interfacial cooling) are identified, and the criterion for utilization of the transient cooling effect is established based on the time constants.

Acknowledgement

This work is supported by the DARPA HERETIC program.

References

[1] Goldsmid HJ. Electronic refrigeration. New York: Plenum Press; 1986.

[2] Stilbans LS, Fedorovich NA. Cooling of thermoelectric cells under nonstationary conditions. Sov Phys Tech Phys 1958;3:460–3.
[3] Parrott JE. Interpretation of stationary and transient behaviour of refrigerating thermocouples. Solid State Electron 1960;1:135–43.
[4] Landecker K, Findlay AW. Study of fast transient behaviour of Peltier junctions. Solid State Electron 1961;2:239–60.
[5] Idnurm M, Landecker K. Experiments with Peltier junctions pulsed with high transient currents. J Appl Phys 1963;34:1806–10.
[6] Babin VP, Iordanishvili EK. Enhancement of thermoelectric cooling in nonstationary operation. Sov Phys Tech Phys 1969;14:293–8.
[7] Hoyos GE, Rao KR, Jerger D. Fast transient response of novel Peltier junctions. Energy Conversion 1977;17:23–9.
[8] Field RL, Blum HA. Fast transient behavior of thermoelectric coolers with high current pulse and finite cold junction. Energy Conversion 1979;19:159–65.
[9] Miner A, Majumdar A, Ghoshal U. Thermoelectromechanical refrigeration based on transient thermoelectric effects. Appl Phys Lett 1999;75:1176–8.
[10] Snyder GJ, Fleurial J-P, Caillat T, Yang RG, Chen G. Supercooling of Peltier cooler using a current pulse. J Appl Phys 2002;92:1564–9.
[11] Hoyos GE, Rao KR, Jerger D. Numerical analysis of transient behavior of thermoelectric coolers. Energy Conversion 1977;17:45–54.
[12] Landecker K. Some further remarks on the improvements of Peltier junctions for thermoelectric cooling. Energy Conversion 1974;14:21–33.
[13] Kumar R, Yang RG, Chen G, et al. Transient thermoelectric cooling of thin film devices. In: Proceedings of the MRS Spring meeting; 2000.
[14] Yang RG, Chen G, Snyder GJ, et al. Geometric effect on the transient cooling of thermoelectric coolers. In: Proceedings of the MRS Fall meeting; 2001.
[15] Volklein F, Blumers M, Schmitt L. Thermoelectric microsensors and microactuators (MEMS) fabricated by thin film technology and micromachining. In: Proceedings of the 18th ICT; 1999. p. 285–93.
[16] Fleurial J-P, Snyder GJ, Herman JA, et al. Thick-film thermoelectric microdevices. In: Proceedings of the 18th ICT; 1999. p. 294–300.
[17] Min G, Rowe DM, Volklein F. Integrated thin film thermoelectric cooler. Electron Lett 1998;34:222–3.
[18] Yao DJ, Kim CJ, Chen G. Design of thermoelectric thin film coolers. In: Proceedings of the international mechanical engineering congress and exhibition, Orlando, FL; 2000.